Fractal structures in chaotic Hamiltonian systems, with applications to plasma physics

Ricardo L. Viana
viana@fisica.ufpr.br

Departamento de Física, Universidade Federal do Paraná, Curitiba-PR, Brasil

V Escola de Verão de Física de Curitiba, Universidade Federal do Paraná, 05 de fevereiro de 2024











Contents

Introduction

Theoretical model

Escape basins

Fractal dimension of the basin boundary

Basin entropy

Wada property

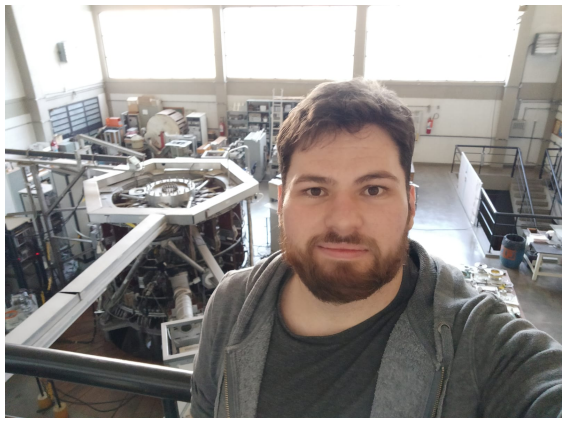
Conclusions

Many thanks to:

- Amanda C. Mathias (Post-Doc, CAPES)



- Leonardo Costa de Souza (PhD student - almost finished!)



- Pedro Haerter Neto (PhD student, now in Madrid/Spain)

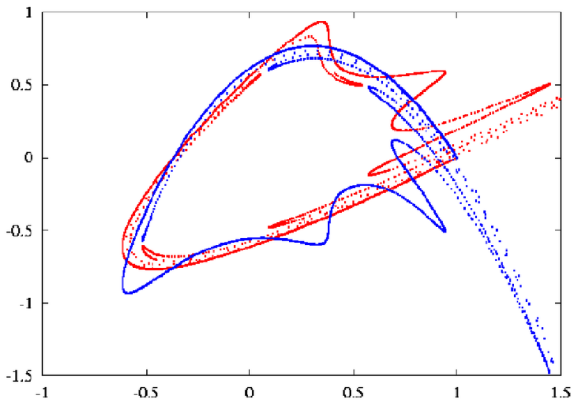


Introduction



- fractals are self-similar geometric objects that do not obey Euclidean geometry
- studied for more than a century: Gaston Julia, Pierre Fatou, Benoit Mandelbrot, ...
- fractals occur often in nonlinear dynamics, both in dissipative and conservative dynamical systems

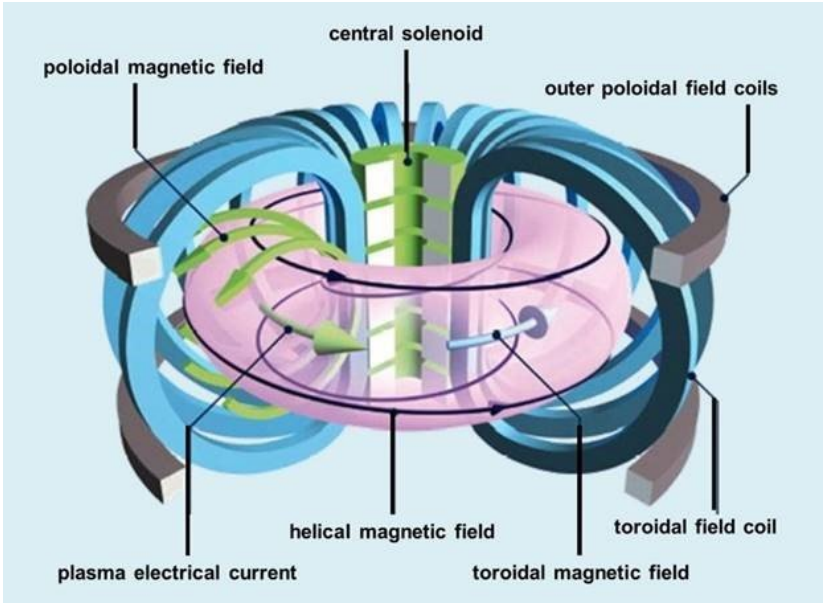
Introduction





- the skeleton of chaotic dynamics is the homoclinic tangle, first described by Henri Poincaré in 1890´s
- the dynamics underlying the homoclinic tangle is based on a non-attracting, chaotic invariant set called Smale horseshoe
- the Smale horseshoe has a fractal structure, that is reflected in the complicated geometry of chaotic attractors and fractal basin boundaries, for dissipative systems
- in open conservative systems, fractal structures are present in escape basins and escape basin boundaries

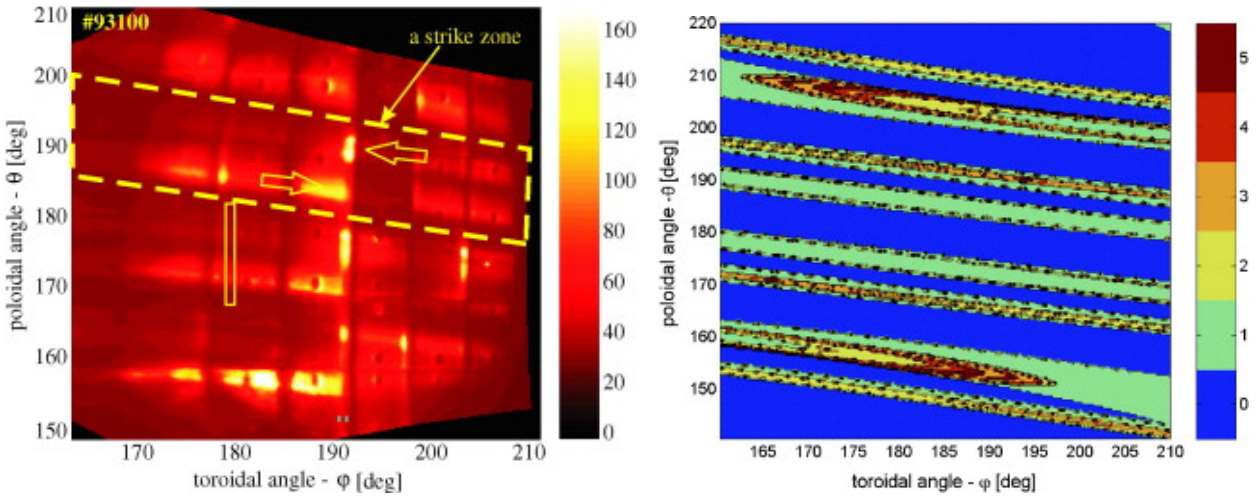
Tokamaks





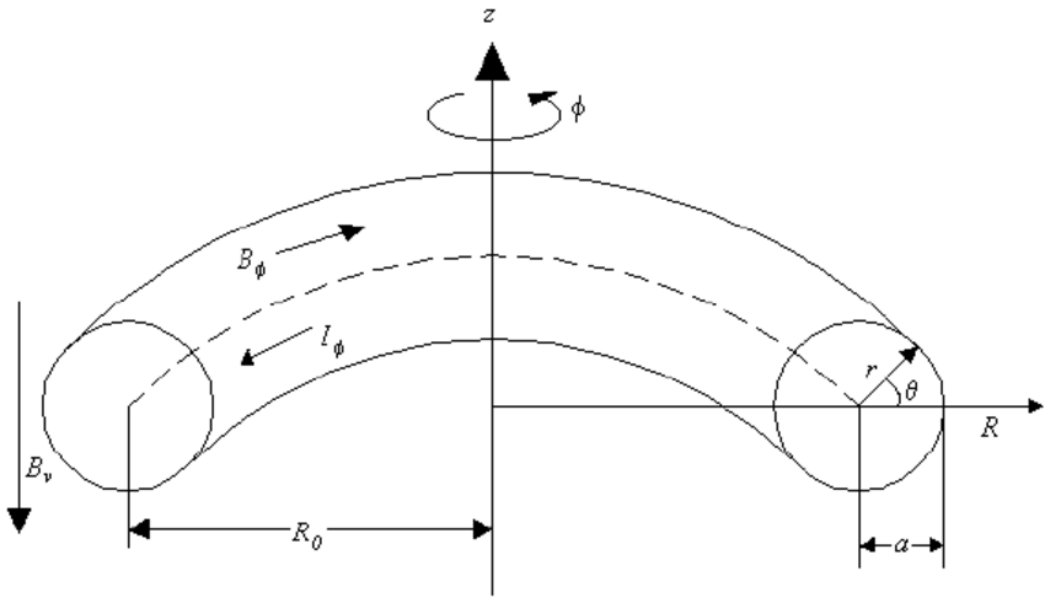
- toroidal systems for the magnetic confinement of fusion plasmas (TCABR Tokamak, Universidade de São Paulo)
- two basic magnetic fields: toroidal (external coils) and poloidal (due to the plasma itself)
- plasma confinement is affected by its interaction with the tokamak wall (divertor plates)

Introduction



- there are experimental evidences of fractal structures in heat deposition patterns in divertor plates of tokamaks [M. Jakubowski *et al.*, J. Nucl. Mat. **337-339**, 176-180 (2005)]
- dynamics of charged particles in combined electric and magnetic fields in tokamak plasmas: non-integrable conservative systems exhibiting chaotic behavior
- we investigate theoretically the existence of fractal structures related to chaotic dynamics of particles in tokamaks

Basic tokamak elements



- local coordinates: (r, θ, φ)
- a, R_0 are the minor and major radii, respectively
- large aspect ratio approximation: $\epsilon = a/R \ll 1$
- equilibrium magnetic field: $\mathbf{B} = (0, B_\theta(r), B_\varphi)$
- Tokamak scaling: $B_\theta \sim \epsilon B_\varphi$, hence $B \approx B_\varphi \gg B_\theta$ and thus consider B as a uniform field
- magnetic surfaces are nested tori with circular cross sections, with safety factor $q(r) = rB/RB_\theta(r)$

Guiding center $\mathbf{E} \times \mathbf{B}$-drift motion

- an applied time-independent electric field in the radial direction, plus a time-dependent field (drift instabilities)

$$\mathbf{E} = \bar{E}_r(r)\hat{\mathbf{r}} - \nabla\tilde{\phi}(r, \theta, \varphi; t).$$

- guiding center equation of motion

$$\frac{d\mathbf{r}}{dt} = v_{\parallel}\frac{\mathbf{B}}{B} + \frac{\mathbf{E} \times \mathbf{B}}{B^2},$$

- $v_{\parallel}$: toroidal plasma velocity
- components in the local coordinate system

$$\begin{aligned}
\frac{dr}{dt} &= -\frac{1}{rB}\frac{\partial\tilde{\phi}}{\partial\theta}, \\
\frac{d\theta}{dt} &= \frac{rv_{\parallel}(r)}{Rq(r)} - \frac{\bar{E}_r(r)}{rB} + \frac{1}{rB}\frac{\partial\tilde{\phi}}{\partial r}, \\
\frac{d\varphi}{dt} &= \frac{v_{\parallel}(r)}{r\sin\theta}
\end{aligned}$$

$\mathbf{E} \times \mathbf{B}$-drift motion

- the electric potential related to the drift instabilities is assumed to exhibit a broad spectrum of frequencies $\omega_n = n\omega_0$

$$\tilde{\phi}(r, \theta, \varphi; t) = \sum_{m,\ell,n} \phi_{m,\ell} \cos(m\theta - \ell\varphi - n\omega_0 t),$$

- retaining only the dominant Fourier mode ($m = M, \ell = L$)

$$\tilde{\phi}(\theta, \varphi; t) = \phi_{ML} \cos(M\theta - L\varphi) \sum_n \delta(\omega_0 t - 2\pi n)$$

- action-angle variables: $I = (r/a)^2$, $\Psi = M\theta - L\varphi$,
- Hamilton's equations for the drift motion

$$\frac{dI}{dt} = -\frac{\partial H}{\partial \Psi} = -\frac{4\pi M \phi_{ML}}{a^2 B \omega_0} \sin\Psi \sum_n \delta(\omega_0 t - 2\pi n),$$

$$\frac{d\Psi}{dt} = \frac{\partial H}{\partial I} = \frac{v_{\parallel}(r)}{R_0 q(r)}(M - qL) - \frac{M \bar{E}_r(I)}{aB\omega_0 \sqrt{I}}.$$

Poincaré map for the $\mathbf{E} \times \mathbf{B}$-drift motion

W. Horton *et al.*, Phys. Plasmas **5**, 3910 (1998);

- stroboscopic sampling of the action-angle variables at integer multiples of the characteristic period

$$I_n = I(t = 2\pi n/\omega_0), \qquad \Psi_n = \Psi(t = 2\pi n/\omega_0),$$

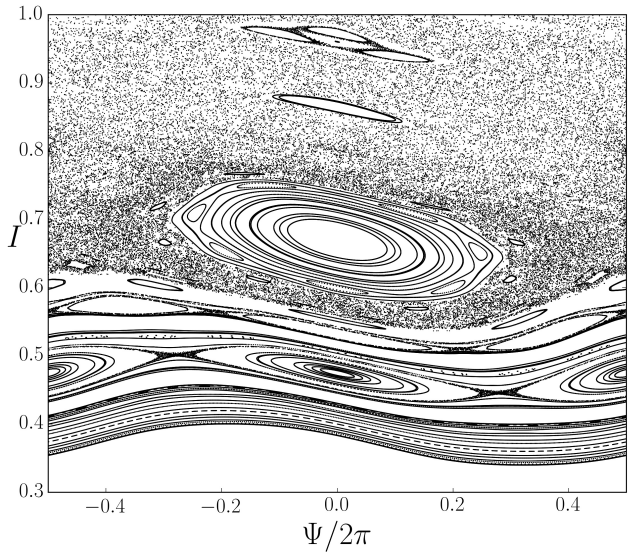
- area-preserving two-dimensional Poincaré map ($\phi_{ML} \equiv \phi$)

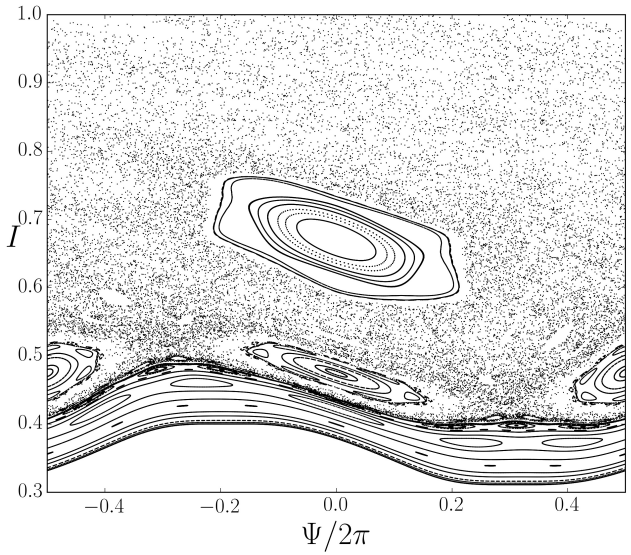
$$I_{n+1} = I_n + \frac{4\pi M \phi}{a^2 B \omega_0} \sin \Psi_n,$$

$$\Psi_{n+1} = \Psi_n + \frac{v_{\|}(I_{n+1})}{\omega_0 R_0} \frac{M - Lq(I_{n+1})}{q(I_{n+1})} - \frac{M}{aB\omega_0} \frac{\bar{E}_r(I_{n+1})}{\sqrt{I_{n+1}}},$$

- parameters taken from tokamak TCABR (University of São Paulo, Brazil): $a = 0.180$ m, $R_0 = 0.615$ m, $B = 1.1$ T,
- all physical quantities have been normalized
- dominant mode: $M = 15$ and $L = 6$, with $\omega_0 = 16.36$.

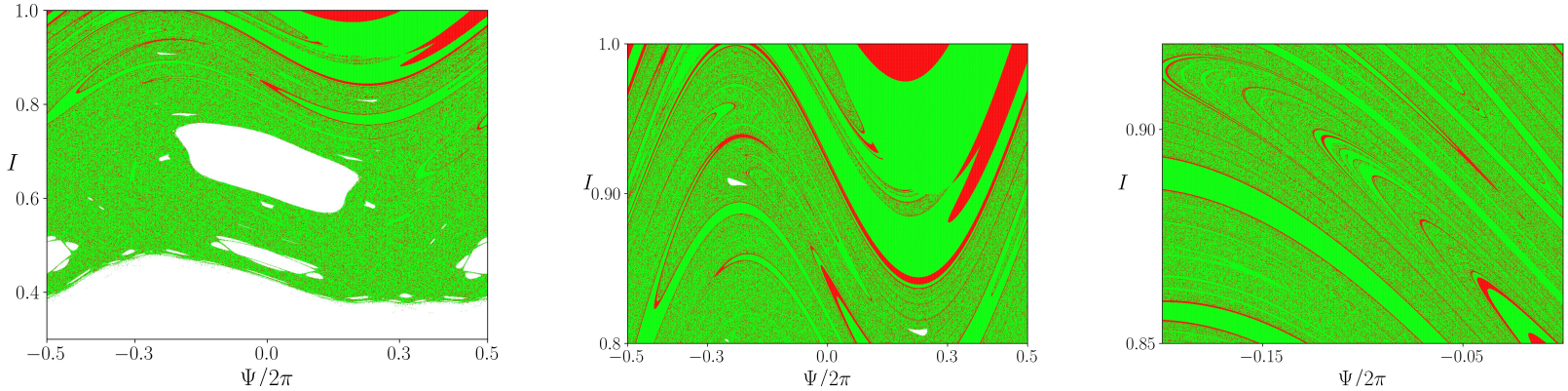
Phase portraits





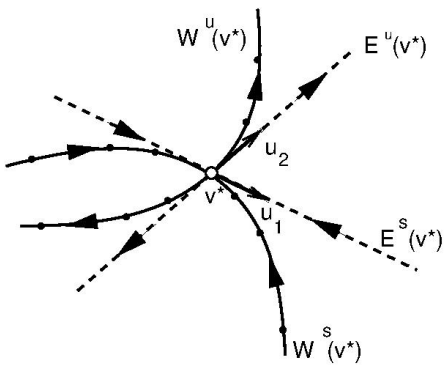
- Poincaré surface of section is the phase plane $I \times \Psi/2\pi$
- (a) $\phi = 4.92 \times 10^{-3}$: divided phase space: quasiperiodic tori, periodic islands, and a large outer chaotic orbit
- (b) $\phi = 7.65 \times 10^{-3}$: chaotic region is predominant over the peripheral plasma column
- condition of escape through the fixed boundary $I = 1$ (in the Poincaré surface of section): $I_n > 1$ for $n \geq 1$

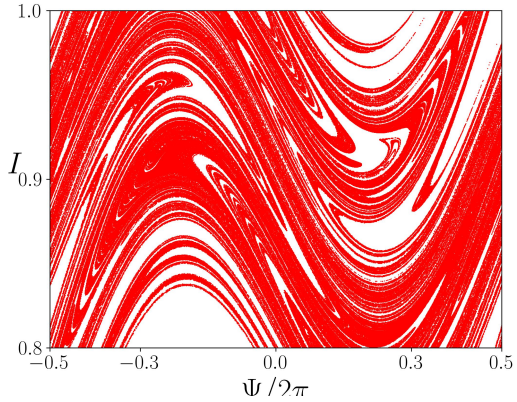
Escape basins

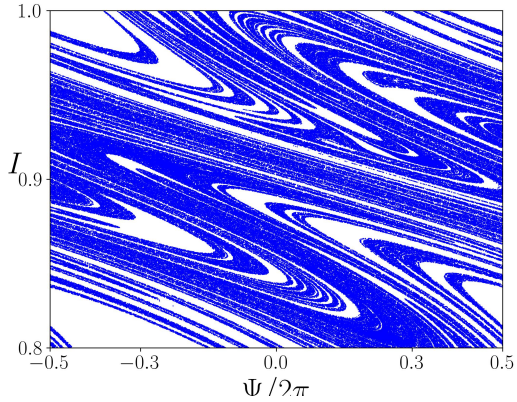


- $\phi = 8.74 \times 10^{-3}$: the boundary line $I = 1$ is divided into two halves (left L and right R of $\Psi = 0$)
- green points: initial conditions of particles escaping through $-0.5 \leq \Psi < 0.0$ ($B(L)$: basin of L exit)
- red points: particles escaping through $0 \leq \Psi \leq 0.5$ ($B(R)$: basin of R exit)
- white points: non-escaping particles (up to a given time limit)
- escape basins are intertwined in arbitrarily fine scales: signature of fractal behavior

Invariant manifolds

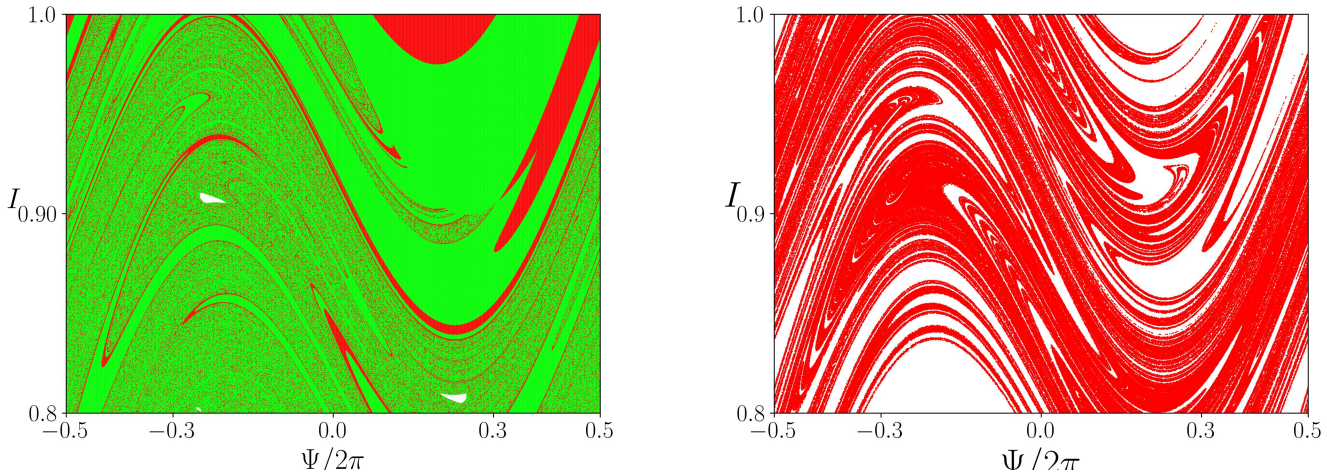






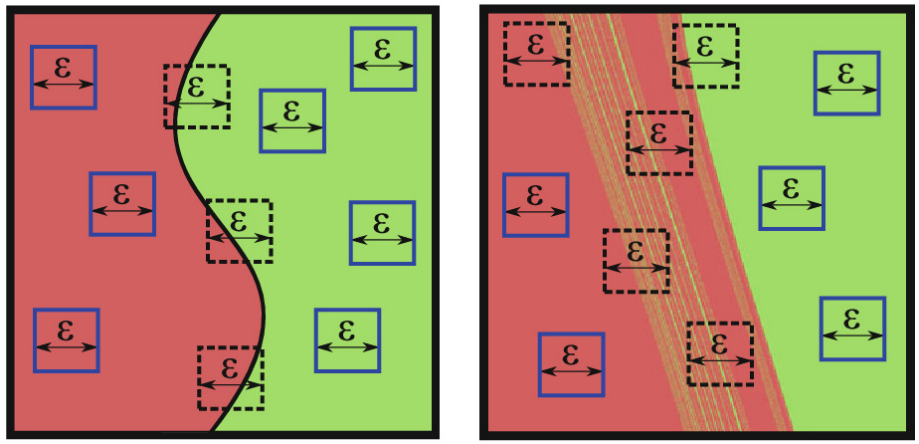
- a typical unstable periodic orbit (saddle point) embedded in a chaotic orbit has two manifolds invariant under the dynamics
- stable manifold: points approaching asymptotically the periodic orbit
- unstable manifold: points move away from the saddle orbit
- invariant manifolds cross transversely at homoclinic points (Henri Poincaré, 1890): fractal structure
- $\phi = 8.74 \times 10^{-3}$: manifolds numerically estimated using the sprinkler method

Invariant manifolds and escape basin boundaries



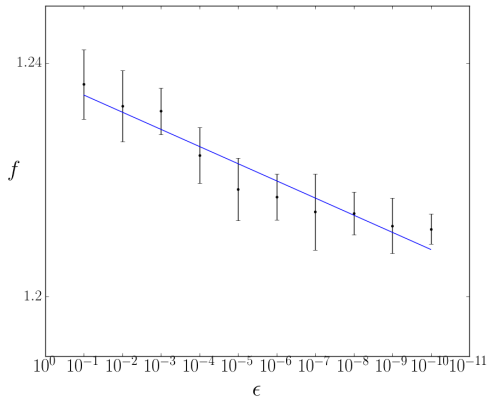
- $\phi = 8.74 \times 10^{-3}$: the boundary between the escape basins (of L and R exits) approach the stable invariant manifold
- the stable manifold is the closure of the escape basin boundary
- there is an accumulation of the escape basin filaments at the stable manifold in the chaotic phase space region
- the escape basin boundary converges to the stable manifold of an unstable periodic orbit embedded in a chaotic orbit

Uncertainty exponent



- ε: initial condition error: sidelength of a box centered at that initial condition (I_0, Ψ_0)
- if an ε-box intercepts the escape basin boundary, the corresponding initial condition is ε-uncertain
- $f(\varepsilon)$: fraction of ε-uncertain boxes randomly chosen in phase space
- if the boundary is smooth, then $f(\varepsilon) \sim \varepsilon$
- if the boundary is fractal, $f(\varepsilon) \sim \varepsilon^{\xi}$, where $0 < \xi < 1$ is the uncertainty exponent
- $\xi = 2 - d$, where d is the box-counting dimension of the escape basin boundary

Numerical determination of the uncertainty exponent



- we randomly choose a large number of initial conditions in the chaotic region
- for each initial condition we determine the escape boundary it belongs (R or L)
- we choose two other initial conditions inside the same ε-box and repeat the test
- if any of these three initial conditions fail to converge to the same exit, the first initial condition is ε-uncertain
- we plot $\ln f(\varepsilon)$ as a function of $\ln \varepsilon$: the uncertainty exponent ξ is the slope of the least-squares fit

Escape basin boundary fractal dimension

ϕ (10^{-3})	ξ	d	error
4.92	0.0001	1.999	0.001
7.65	0.0011	1.999	0.001
8.74	0.0034	1.997	0.002
10.38	0.0157	1.980	0.030

- the escape basin boundary dimension is nearly equal to $2,0$ for all values of the perturbation strength
- similar to area-filling curves (like Peano curve, 1890)
- since $\alpha \approx 0$ no improvement in reducing the error ε will produce a decrease in the uncertain fraction of initial condition
- catastrophic final-state uncertainty: it is virtually impossible to predict by which exit will a particle escape
- however, the box-counting dimension of the fractal escape basin boundary is not a good quantifier of final-state uncertainty: other methods are needed.

Basin entropy

A. Daza *et al.*, Sci. Rep. **6**, 31416 (2016)

- we cover a phase space region Ω by a fine mesh of boxes of size ε
- to each grid point we assign a random variable with the different exits as the possible outcomes
- to each initial condition in a given box we assign a variable ("color") labeled from 1 to N_A
- the colors within each box are randomly distributed according to a probability $p_{i,j}$ for the jth color assigned to the ith box
- on supposing that the trajectories inside a box are statistically independent we compute the Gibbs entropy of the ith box as

$$S_i = -\sum_{j=1}^{m_j} p_{i,j} \log p_{i,j}$$

- where $m_i \in [1, N_A]$ is the number of colors inside the ith box.
- the entropy of the whole grid is computing by the addition of the entropy of each of the N boxes $S = \sum_{i=1}^{N} S_i$

Basin boundary entropy

- relative basin entropy $S_b = S/N$: measures the uncertainty degree of an escape basin
- a single exit: $p_{i,j} = 1$ hence $S_b = 0$
- completely randomized escape basins with N_A equiprobable exits: $S_b = \log N_A$
- basin boundary entropy: $S_{bb} = S/N_b$, where N_b is the number of boxes which contain more than one color
- those are the boxes falling in the boundaries
- S_b is sensitive to the size of the basins, but S_{bb} is not
- the maximum possible value of S_{bb} that a smooth boundary can show is $\log N_A$
- if $S_{bb} > \log N_A$ then the boundary is fractal
- this is a sufficient but not necessary condition: there may be fractal boundaries with $S_{bb} < \log N_A$

Escape basin entropy

- choose Ω to be inside a chaotic region in the phase plane $I \times \Psi$, for a given value of the perturbation strength ϕ
- $N_A = 2$ exits: L ($\Psi < 0$, green basin) and R ($\Psi > 0$, red basin)
- cover Ω with a $10^3 \times 10^3$ grid and, for each box we randomly choose 1000 initial conditions (I_0, Ψ_0), and iterate each one for 1000 times (maximum)
- $n_L(n_R)$: number of points of the box corresponding to particles escaping through exit L (R)

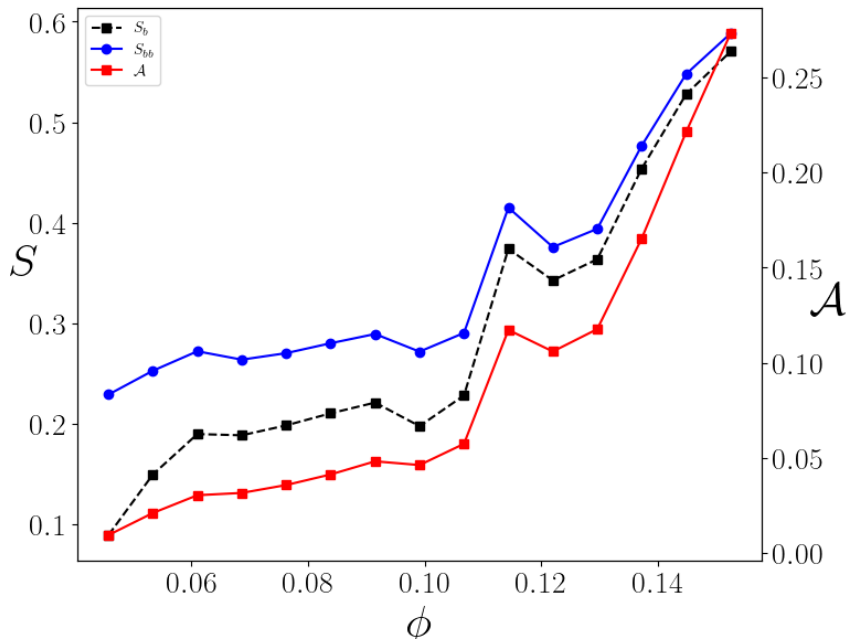
$$p_L = \frac{n_L}{n_R + n_L}, \qquad p_R = \frac{n_R}{n_R + n_L}$$

- compute the entropy S_i of each box

$$S_i = -p_L \log p_L - p_R \log p_R$$

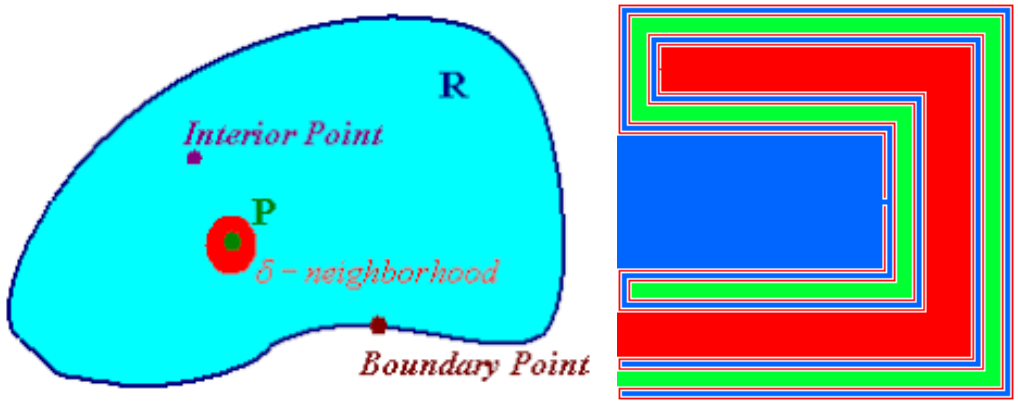
- basin entropy: $S_b = (1/N) \sum_i S_i$
- basin boundary entropy: S_{bb} considers only those those boxes for which either $p_L = 0$ or $p_R = 0$: there were considered only those boxes which have at least one boundary in their interior

Escape basin and basin boundary entropies



- the basin entropy increases, as a trend, with the perturbation strength ϕ
- for large perturbation it almost reaches its theoretical maximum $\log 2 \approx 0.69$: practically equiprobable escape basins
- the basin boundary entropy is always smaller than the basin entropy: the number of boxes containing points of the boundary is less than the total number of boxes

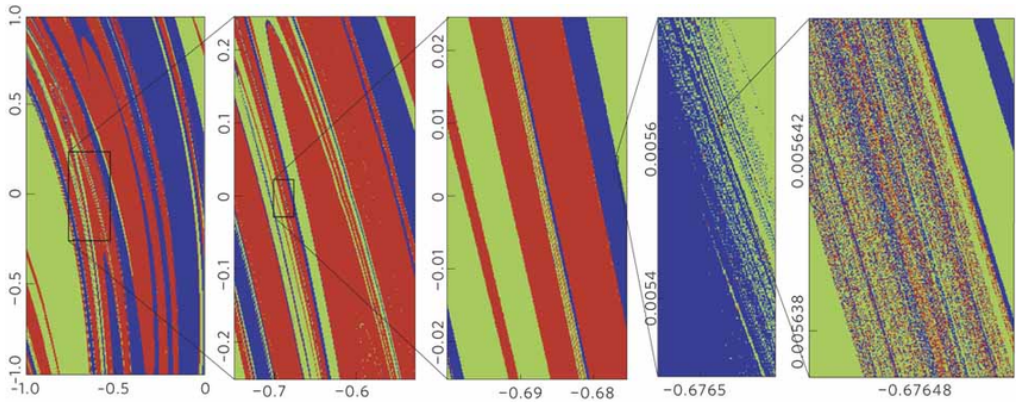
Wada property



- a point P is a boundary point of an escape basin B if every open neighborhood of P intersects the basin B and at least another basin $B' \neq B$
- the basin boundary is the set of all boundary points of that escape basin
- the boundary point P is also a Wada point if every open neighborhood of P intersects at least three different basins
- a basin boundary possess the Wada property if every boundary point of B is a Wada point, such that the boundary of such a basin is a Wada exit basin boundary (Koneyama, 1917)

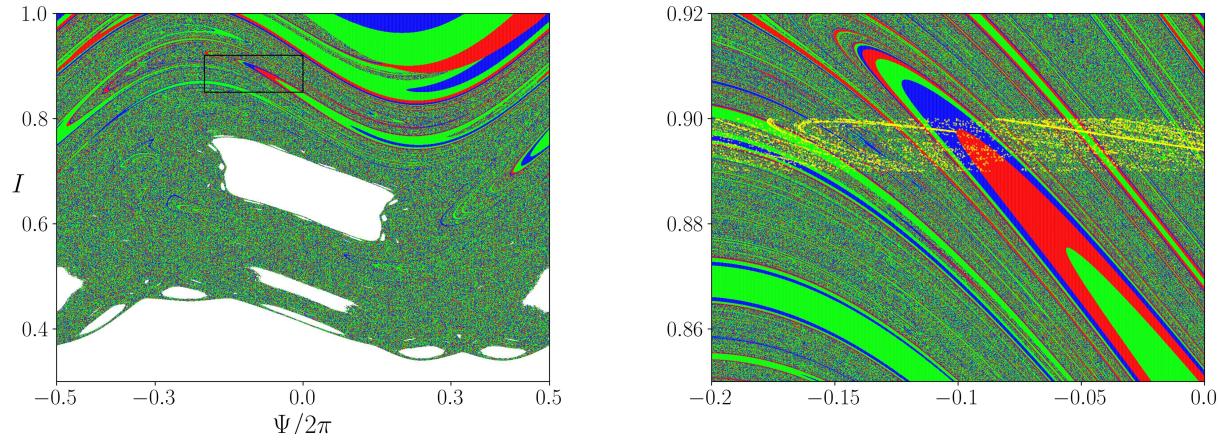
Wada basins





- an example of Wada point is the "three frontier mark": point where the frontiers between Brazil, Argentina and Paraguay meet together (in state of Paraná)
- for smooth boundaries these are exceptional points
- for fractal boundaries the Wada property may hold partially or totally
- extreme final-state sensitivity, for three or more escape basins with the Wada property

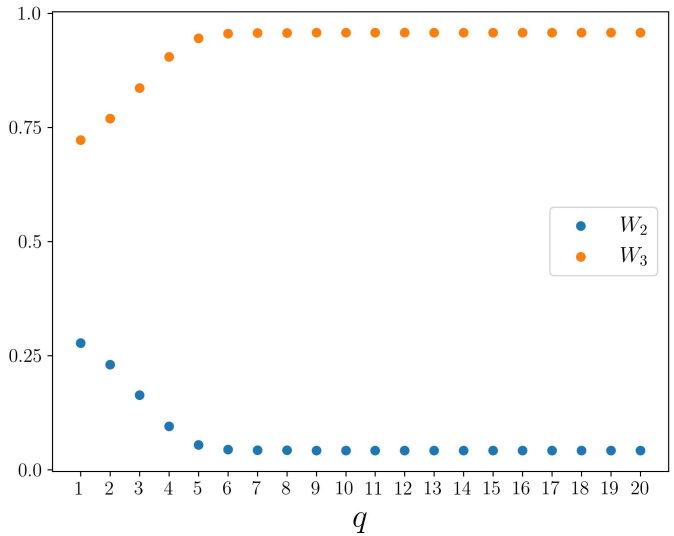
Wada escape basins



- now we have three exits at the boundary line $I = 1$:
  1. L: $-\pi < \Psi \leq -\pi/3$: red points
  2. C: $-\pi/3 < \Psi \leq \pi/3$: blue points
  3. R: $\pi/3 < \Psi \leq \pi$: green points
- a magnification of a rectangle containing pieces of the three exit basins, suggests that stripes of all basins coexist in increasingly finer scales
- basic test for the Wada property: the unstable manifold of a periodic orbit (white line) intersects all the escape basins (this is a necessary but not sufficient condition): yellow points

Quantifying Wada property

A. Daza *et al.*, Sci. Rep. **5**, 16579 (2015)



- three classes: G_1: internal points, G_2: boundary points between two basins, G_3: boundary points between three basins (Wada property)
- we compute the fraction of points of each category using a refinement numerical procedure
- $W_2 = 0$: no Wada property; $0 < W_2 < 1$: partial Wada property; $W_2 = 1$: full Wada property

Conclusions

- the escape basins are fractal, and the fractal dimension of the escape basin boundary is nearly 2.0 (almost an area-filling curve)
- extreme final-state uncertainty: no reduction of the error in the initial condition determination can improve our ability to predict by which exit will a given particle escape through
- the escape basin entropy (and the basin boundary entropies) increase with the intensity of electrostatic fluctuations
- Wada property: holds for three or more escape basins. A given boundary point has neighborhoods with points belonging to all basins
- for three exits (at the boundary line) we verify the presence of Wada property qualitatively
- the Wada property holds for nearly 96% of the escape basin boundary points



- L. C. de Souza, M. R. Sales, M. Mugnaine, J. D. Szezech Jr., I. L. Caldas, R. L. Viana, Phys. Rev. E **109**, 015202 (2024)
- L. C. de Souza, A. C. Mathias, I. L. Caldas, Y. Elskens, and R. L. Viana, Chaos **33**, 083132 (2023)
- A. C. Mathias, L. C. de Souza, A. B. Schelin, I. L. Caldas, and R. L. Viana, J. Appl. Nonlin. Dyn. **12**, 723 (2023)
- P. Haerter, L. C. de Souza, A. C. Mathias, R. L. Viana, and I. L. Caldas, Int. J. Bifurcat. Chaos **33**, 2330022 (2023)
- L. C. de Souza, A. C. Mathias, P. Haerter, R. L. Viana, Entropy **25**, 1142 (2023)
- J. Aguirre, R. L. Viana, and M. Sanjuán, Rev. Mod. Phys. **81**, 333 (2009)